Journal of the Franklin Institute 361 (2024) 106838

Contents lists available at ScienceDirect

Journal of the Franklin Institute

journal homepage: www.elsevier.com/locate/fi

# Adaptive-frequency event-based approach to finite horizon state estimation for complex networks using multi-channel random access protocol

Jinzhao Miao [a], Lijuan Zha [b,*], Jinliang Liu [c], Xiangpeng Xie [d], Engang Tian [e]

[a] College of Information Engineering, Nanjing University of Finance and Economics, Nanjing, 210023, Jiangsu, China
[b] College of Science, Nanjing Forestry University, Nanjing, 210037, Jiangsu, China
[c] School of Computer Science, Nanjing University of Information Science and Technology, Nanjing, 210044, Jiangsu, China
[d] Institute of Advanced Technology, Nanjing University of Posts and Telecommunications, Nanjing, 210023, Jiangsu, China
[e] School of Optical-Electrical and Computer Engineering, University of Shanghai for Science and Technology, Nanjing, 200093, Jiangsu, China

ARTICLE INFO

*Keywords:*
Complex networks (CNs)
Event-triggered mechanism (ETM)
Multi-channel random access protocol (MRAP)
State estimation

ABSTRACT

The issue of $H_\infty$ state estimation is addressed for complex networks (CNs) with inner coupling disturbance (ICD) while utilizing adaptive-frequency event-triggered mechanism (AFETM) and multi-channel random access protocol (MRAP). To maintain transmission frequency as much as possible while reducing data transmission, the proposed AFETM dynamically modifies the threshold based on the historical number of transmissions within a defined time interval. Data transmission after AFETM is scheduled by the MRAP, which enables the random selection and transmission of multiple signals, thereby avoiding network conflicts and congestion. The primary objective is to devise a estimator that guarantees the estimation errors meet the prescribed $H_\infty$ performance. The attainment of sufficient conditions to achieve this objective involves the utilization of stochastic analysis. On this basis, the expected estimator gain is determined through the solution of the backward coupled difference equations. Ultimately, the performance of the devised estimator is validated by simulation.

## 1. Introduction

Complex networks (CNs) are network structures composed of many nodes and connections, possessing many characteristics that do not exist in traditional networks [1–3], including self-organization, robustness, and adaptability [4]. In fields such as machine learning, data mining, artificial intelligence, CNs find extensive applications in tasks such as text classification, recommendation systems, and image recognition to accelerate data processing and analysis [5–7]. The extensive application of CNs in biology, physics, sociology, computer science, and other fields highlights the importance of researching CNs. By analyzing the structure and properties of CNs, one can better understand information propagation, dynamic evolution, and related phenomena [8]. CNs provide a novel method for researching and simulating complex real-world systems.

Obtaining the state of nodes is one of the fundamental challenges encountered in the application of CNs. However, direct acquisition of state can only be achieved in networks with relatively simple dynamic behaviors and small number of nodes [9]. The state of large-scale CNs is often impossible to obtain directly through measurement [10]. The usual solution is to use the measurable output data to estimate the unmeasurable state information, which is also the core issue discussed in this paper.

* Corresponding author.
*E-mail address:* zhalijuan@vip.163.com (L. Zha).

https://doi.org/10.1016/j.jfranklin.2024.106838
Received 12 December 2023; Received in revised form 4 March 2024; Accepted 11 April 2024
Available online 20 April 2024
0016-0032/© 2024 The Franklin Institute. Published by Elsevier Inc. All rights reserved.

In [11], the nonfragile estimation method is explored for CNs with switching topologies using quantized signal processing. A research investigation is presented on the state estimation approach for CNs characterized by stochastic variations in topology subject to variance constraints in [12]. However, these estimation schemes are based on relatively ideal network environments, and when applied to practical issues, they may be invalid and result in reduction of estimation accuracy due to unconsidered external factors [13], which makes the estimation problem in complex environments more valuable. While ensuring that the estimation error is within an acceptable range, this paper will further propose estimation strategies with stronger robustness and stability from the more realistic perspectives of external perturbations and network resource limitations.

The coupling between nodes in CNs refers to the interaction relationships between different nodes in the network [14–16]. In CNs, nodes can be coupled to each other in various ways, such as physical connections, information transmission, and energy transfer. The coupling relationships between nodes in a complex network form the basis of network structure formation, which determines various dynamic behaviors and evolutionary patterns of the network [17,18]. Therefore, in-depth research on the coupling relationships between nodes in a complex network is of great significance for understanding the structure and function of the network. Currently, the coupling relationships in related research are assumed to be already determined, but some papers point out that the actual coupling relationships in complex networks are not accurate, which has attracted a group of researchers to further study uncertain couplings. In [19], a recursive state estimation scheme under variance constraints is discussed for CNs with uncertain inner couplings and measurement signals processed using quantization techniques. In consideration of the situations involving event-triggered mechanism (ETM) and state saturation, a filtering method is proposed for CNs with random coupling strengths in [20]. This paper will design an estimator considering inner coupling disturbance (ICD) to enhance the robustness of estimator.

Due to the property of including many nodes, CNs are prone to generating large amounts of data traffic in a short period of time, which can result in network congestion and conflicts and seriously affect normal communication [21,22]. Many studies have been conducted to solve network conflict issues using ETM [23–26], which aim to reduce unnecessary signal transmission [27]. For example, the filtering problem is investigated for CNs in [28], where multiple ETMs regulate communication between nodes. To effectively regulate signal transmission in the event of significant fluctuations in sensor data, dynamic event-triggered mechanism (DETM) with dynamic thresholds has been proposed [29–31]. The pinning synchronization for CNs with switched impulsive dynamics and asynchronous switching is discussed in [32] under the influence of DETM. A filtering method for CNs with switching topology influenced by DETM and random sensor failures is studied in [33]. However, even with the use of DETM to regulate data transmission, it is still challenging to ensure the generation of stable transmission frequencies that are crucial for reducing network congestion [34]. In order to further reduce the likelihood of complex network transmitting large amounts of data in a short period of time, an adaptive frequency event-triggered mechanism has been proposed based on the DETM. AFETM adaptively adjusts the triggering threshold based on the event trigger frequency in the past period of time, aiming to stabilize the trigger frequency and avoid frequent triggering within a short period of time that may cause data flow impact on network stability.

Recently, another data transmission control method utilizing communication protocols has gained attention [35,36]. The common scheduling approach in current communication protocols is to select data from one node at a time for transmission [37]. Common communication protocols include random access protocol (RAP) [38,39], round-robin protocol (RRP) [40–42], and weight try-once-discard protocol [43–45]. Currently, some communication protocols have been employed to mitigate network congestion. The estimation method of CNs with sensor saturation under RAP is investigated in [46] based on partial node information. The $H_\infty$ state estimation problem of CNs with nonlinear singular perturbations and RRP is discussed in [47]. Among communication protocols, RAP is simple to implement and widely used in industrial practical problems, and therefore is also an important research object. Its main principle is to randomly select signal of one node transmission at each moment. It is demonstrated as an effective method for mitigating network conflict, but the significant reduction in the amount of transmitted data diminishes the performance of the estimator. In order to control the estimation error within an acceptable range, the amount of transmitted data should be appropriately increased, and thus the multi-channel random access protocol (MRAP) that uses multiple channels to transmit signals simultaneously will be proposed. MRAP selects signals from multiple nodes for transmission at each moment. By adjusting the number of occupied channels, it can balance the performance of the estimator and network transmission amount. The estimator designed based on MRAP in this paper has better performance than general RAP, under the premise of effectively solving network congestion problems.

Based on the aforementioned discussion, this paper investigates the estimation problem of CNs with ICD under limited network bandwidth. The AFETM and MRAP are implemented to mitigate network congestion and conflicts caused by limited network communication resources. The distinguishing innovations of the main results are characterized by the following aspects: (1) The state estimation of CNs with ICD under the simultaneous influence of AFETM and MRAP is explored for the first time. (2) To tackle the challenge posed by limited network resources, AFETM is proposed, which can dynamically adjust the threshold to maintain a stable transmission frequency. In addition, MRAP that enables the random selection and transmission of measurements from multiple nodes is introduced. (3) The adequate conditions for guaranteeing that the dynamic estimation errors satisfy the $H_\infty$ performance are obtained through the utilization of random analysis techniques and solving backward coupled difference equations.

## 2. Problem formulation

### 2.1. System description

The dynamics of CNs with $N$ coupled nodes are described as

$$\begin{cases} x_i(k+1) = A_i(k)x_i(k) + \sum_{j=1}^{N} \omega_{ij}(\Gamma + \tilde{\Gamma})x_j(k) + B_i(k)v_i(k) \\ y_i(k) = C_i(k)x_i(k) + D_i(k)v_i(k) \\ z_i(k) = H_i(k)x_i(k) \end{cases} \tag{1}$$

where $x_i(k) \in \mathbb{R}^n (i = 1, 2, \dots, N)$ denotes the state of $i$th node for $k \in [0, T]$. $y_i(k) \in \mathbb{R}^m$ and $z_i(k) \in \mathbb{R}^m$ stand for the measurement output and the output to be estimated, respectively. $v_i(k)$ denotes the external disturbances. $W = (\omega_{ij})_{N\times N}$ with $\omega_{ij} \geq 0 (i \neq j)$ is the coupling configuration matrix, where $\omega_{ij} = \omega_{ji}$ and $\omega_{ii} = -\sum_{j=1, j\neq i}^{N} \omega_{ij}$. $\Gamma = \mathrm{diag}_{1\leq i\leq N}\{\gamma_i\}$ is the inner coupling matrix with $\gamma_i > 0$, and $\tilde{\Gamma} = \mathrm{diag}_{1\leq i\leq N}\{\tilde{\gamma}_i\}$ is the coupling disturbance. The expectation of independent random variables $\tilde{\gamma}_i$ is 0, and its variance is $\beta_i$. $A_i(k), B_i(k), C_i(k), D_i(k)$ and $H_i(k)$ are bounded and known matrices.

### 2.2. Adaptive-frequency event-triggered mechanism

For reducing the data transmission burden on the communication network between sensors and remote estimators, an adaptive-frequency event-triggered mechanism based on the trigger frequency is used to make the determination of whether or not to transmit the current measurement value.

Define the triggering instant sequence as $s(0) < s(1) < \cdots < s(t) < \cdots < T$, and the following threshold function

$$\mathcal{M}(k, \delta(k)) = \|\xi(k)\| - (\theta\delta(k) + \varpi)\|y(k)\|, \tag{2}$$

in which

$$\xi(k) = y(k) - y(s(t)), \quad \delta(k) = \frac{T(p)}{T(r) + T(p)},$$
$$T(\varsigma) = \frac{s(t) - s(t-\varsigma)}{\varsigma}, \quad \varsigma = r, p.$$

The positive scalars $\theta$ and $\varpi$ are given parameters. $s(t)$ being the latest triggering instant before time $k$.

The measurement output $y(k)$ can be triggered and accessible to the communication network only when $\mathcal{M}(k, \delta(k)) \geq 0$. Specifically, the update rule for the next moment of transmission is

$$s(t+1) = \min\{k \mid k > s(t), \mathcal{M}(k, \delta(k)) \geq 0\}. \tag{3}$$

By employing AFETM, the actual triggered signal $\tilde{y}(k)$ is denoted as

$$\tilde{y}(k) = y(s(t)), \quad \forall k \in [s(t), s(t+1)). \tag{4}$$

**Remark 1.** The recent triggering interval $T(r)$ represents the time interval of the latest $r$ signal transmissions. Typically, $r$ is set to be a small value to reflect the frequency of recent signal transmissions. Similarly, the average triggering interval $T(p)$ represents the time interval of the previous $p$ signal transmissions. It is necessary to set $p$ to be a larger value to reflect the frequency of signal transmissions over a longer period of time. The core idea of AFETM is that $T(r)$ dynamically approaches $T(p)$ under the influence of adaptive threshold $\delta(k)$, resulting in a more stable triggering frequency compared to conventional ETM.

**Remark 2.** If $T(r)$ is smaller than $T(p)$, it signifies a higher frequency of signal transmissions in the previous moment $k-1$. From the calculation method of the dynamic threshold $\delta(k)$, it can be inferred that $\delta(k)$ will be greater than $\delta(k-1)$, thereby making it more difficult for AFETM to meet the triggering condition $\mathcal{M}(k, \delta(k)) \geq 0$ and consequently reducing the frequency of signal transmission. Conversely, if $T(r)$ is greater than $T(p)$, it indicates a lower frequency of signal transmissions. As a result, $\delta(k)$ will be smaller than $\delta(k)$, facilitating the occurrence of signal transmission, which contributes to enhancing the performance of estimator. Through adaptively adjusting the threshold to stabilize the triggering frequency of AFETM, more stable data transmission and better estimator performance on average can be achieved.

### 2.3. Multi-channel random access protocol

To reduce communication pressure, MRAP are used in network to determine which signals of nodes can be transmitted. Compared with traditional RAP that only select one node each time, the MRAP considered here can select $a (1 < a < N)$ nodes at each moment.

Define $\tilde{y}(k) = \mathrm{col}_N\{\tilde{y}_i(k)\}$. Let $\sigma_i(k)$ represents whether the $i$th node is selected and $\sum_{i=1}^{N} \sigma_i(k) = a$. Assuming that each node is considered to have an equal weight in terms of selection. The probability of $\sigma_i(k)$ being selected is given by

$$\mathrm{Prob}\{\sigma_i(k) = 1\} = \frac{a}{N}, \quad \mathrm{Prob}\{\sigma_i(k) = 0\} = 1 - \frac{a}{N},$$

where $\sigma_i(k) = 1$ means that the $i$th node can transmit signals, otherwise it cannot transmit.

Denote $\bar{y}(k) = \mathrm{col}_N\{\bar{y}_i(k)\}$ as the measurement output received by the remote estimation. Adopting the zero-order holder strategy, we have

$$\bar{y}(k) = \Phi_{\sigma(k)}\tilde{y}(k) + \left(I - \Phi_{\sigma(k)}\right)\bar{y}(k-1) \tag{5}$$

where $\Phi_{\sigma(k)} = \mathrm{diag}_{1\le i\le N}\left\{\sigma_i(k) I_m\right\}$.

**Remark 3.** Currently, the widely used RAP for addressing network congestion issues randomly sends data of single node at each moment. Although frequent package collisions are avoided, it also has a considerable adverse effect on the performance of the estimator. In CNs, network resources are often insufficient to support data transmission from all sensors, but there are enough network resources to send some data. To fully utilize the existing network resources, MRAP has been introduced, which can specify the number of channels occupied by the scheduling signal according to the specific network environment, balancing the conflict relationship between limited network resources and estimator performance.

**Remark 4.** Compared to the existing state estimation for CNs [11,47], this study considers AFETM with dynamic thresholds and MRAP that fully utilize network resources. The basic difference between the AFETM proposed in this paper and the ETM in [32,33] is that the threshold function in (2) is time-varying and can be adjusted adaptively according to the triggering frequency. The MRAP can adjust the number of transmitted measurement outputs from sensor nodes based on the network environment, which allows for the optimal utilization of currently idle communication channels.

### 2.4. State estimator design

Based on the AFETM (2) and the MRAP (5), the state estimator for CNs (1) is constructed as

$$\begin{cases} \hat{x}_i(k+1) = \left(A_i(k) - L_i(k)C_i(k)\right)\hat{x}_i(k) + \sum_{j=1}^{N}\omega_{ij}\Gamma\hat{x}_j(k) + L_i(k)\bar{y}_i(k) \\ \hat{z}_i(k) = H_i(k)\hat{x}_i(k) \end{cases} \tag{6}$$

where $\hat{x}_i(k)$ and $\hat{z}_i(k)$ are the estimation of $x_i(k)$ and $z_i(k)$, respectively. $L_i(k)$ is the estimation gain matrix.

Denote $e_i(k) = x_i(k) - \hat{x}_i(k)$, $\tilde{z}_i(k) = z_i(k) - \hat{z}_i(k)$, $x(k) = \mathrm{col}_N\{x_i(k)\}$, $e(k) = \mathrm{col}_N\{e_i(k)\}$, $\tilde{z}(k) = \mathrm{col}_N\{\tilde{z}_i(k)\}$, $\upsilon(k) = \mathrm{col}_N\{\upsilon_i(k)\}$, and $\eta(k) = \begin{bmatrix} x^T(k) & \bar{y}^T(k-1) & e^T(k)\end{bmatrix}^T$, then the estimation error system is

$$\begin{cases} \eta(k+1) = \bar{\mathcal{W}}(k)\eta(k) + C(k)\xi(k) + \mathcal{B}(k)\upsilon(k) \\ \tilde{z}(k) = \mathcal{H}(k)\eta(k) \end{cases} \tag{7}$$

where

$$\begin{aligned}
&\bar{A}(k) = \tilde{A}(k) - L(k)C(k), \quad \tilde{A}(k) = A(k) + W\otimes\Gamma, \\
&\bar{\mathcal{W}}(k) = \mathcal{A}(k) + \mathcal{W}(k), \quad \tilde{L}(k) = L(k)(I - \Phi_{\sigma(k)}), \\
&\tilde{B}(k) = B(k) - L(k)\Phi_{\sigma(k)}D(k), \\
&Y = \mathrm{diag}_{1\le i\le N}\{Y_i\}, \quad Y = A(k), L(k), C(k), H(k), B(k), D(k), \\
&\mathcal{A}(k) = \begin{bmatrix} \tilde{A}(k) & 0 & 0 \\ \Phi_{\sigma(k)}C(k) & I - \Phi_{\sigma(k)} & 0 \\ \tilde{L}(k)C(k) & -\tilde{L}(k) & \bar{A}(k) \end{bmatrix}, \\
&\mathcal{W}(k) = \begin{bmatrix} W\otimes\tilde{\Gamma} & 0 & 0 \\ 0 & 0 & 0 \\ W\otimes\tilde{\Gamma} & 0 & 0 \end{bmatrix}, \quad C(k) = \begin{bmatrix} 0 \\ -\Phi_{\sigma(k)} \\ L(k)\Phi_{\sigma(k)} \end{bmatrix}, \\
&\mathcal{B}(k) = \begin{bmatrix} B(k) \\ \Phi_{\sigma(k)}D(k) \\ \tilde{B}(k) \end{bmatrix}, \quad \mathcal{H}(k) = \begin{bmatrix} 0 & 0 & H(k) \end{bmatrix}.
\end{aligned}$$

In this paper, we aim to construct the state estimator (6) for the CNs (1) with the ICD under the simultaneous influence of AFETM (2) and MRAP (5) such that the resulting augmented estimation error dynamics (7) satisfy the following $H_\infty$ performance index:

$$\mathbb{E}\left\{\sum_{k=0}^{T}\mathcal{J}_1(k)\right\} = \sum_{k=0}^{T}\mathbb{E}\left\{\|\tilde{z}(k)\|^2 - \gamma^2\|\upsilon(k)\|^2\right\} < \eta^T(0)S\eta(0) \tag{8}$$

for a prescribed disturbance attenuation level $\gamma > 0$ over a finite-time horizon $[0, T]$, where $S > 0$ is a weighted matrix and $\eta(0)$ is any given non zero initial condition.

## 3. Main results

In this part, we utilize the stochastic analysis to derive the sufficient conditions satisfying the expected performance requirement based on (7).

**Theorem 1.** *Given $\gamma > 0$, $\alpha > 0$, matrix $S^T = S > 0$, and the estimator gain $L(k)$, the estimation error system (7) satisfies the $H_\infty$ performance if there exists matrices $R(k) > 0$ such that the backward difference equations (BDEs) hold for $k \in [0, T]$:*

$$R(k) = \Pi_{3,k+1} + \Theta_{1,k+1}^T \Omega_{2,k+1}^{-1} \Theta_{1,k+1} \tag{9}$$

*with $R(T+1) = 0$ and*

$$\Omega_{1,k+1} > 0, \quad \Omega_{2,k+1} > 0, \quad R(0) < \gamma^2 S \tag{10}$$

*where*

$$\begin{aligned}
\Pi_{3,k+1} &= \tilde{\mathcal{A}}^T(k)\Xi_{k+1}\tilde{\mathcal{A}}(k) + \tilde{\mathcal{W}}^T(k)R(k+1)\tilde{\mathcal{W}}(k) \\
&\quad + \mathcal{H}^T(k)\mathcal{H}(k) + \tilde{\alpha}\bar{C}^T(k)\bar{C}(k), \\
\Xi_{k+1} &= R(k+1) + R(k+1)\tilde{C}(k)\Omega_{1,k+1}^{-1}\tilde{C}^T(k)R(k+1), \\
\Theta_{1,k+1} &= \tilde{\mathcal{B}}^T(k)\Xi_{k+1}\tilde{\mathcal{A}}(k) + \tilde{\alpha}D^T(k)\bar{C}(k), \\
\Omega_{1,k+1} &= \alpha^2 I - \tilde{C}^T(k)R(k+1)\tilde{C}(k), \\
\Omega_{2,k+1} &= \gamma^2 I - \tilde{\mathcal{B}}^T(k)\Xi_{k+1}\tilde{\mathcal{B}}(k) - \tilde{\alpha}D^T(k)D(k), \\
\tilde{\mathcal{A}}(k) &= \begin{bmatrix} \tilde{A}(k) & 0 & 0 \\ \bar{\Phi}C(k) & I - \bar{\Phi} & 0 \\ \bar{L}(k)C(k) & -\bar{L}(k) & \bar{A}(k) \end{bmatrix}, \\
\tilde{\mathcal{W}}(k) &= \begin{bmatrix} W \otimes \bar{\Gamma} & 0 & 0 \\ 0 & 0 & 0 \\ W \otimes \bar{\Gamma} & 0 & 0 \end{bmatrix}, \quad \tilde{C}(k) = \begin{bmatrix} 0 \\ -\bar{\Phi} \\ L(k)\bar{\Phi} \end{bmatrix}, \\
\tilde{\mathcal{B}}(k) &= \begin{bmatrix} B(k) \\ \bar{\Phi}D(k) \\ B(k) - L(k)\bar{\Phi}D(k) \end{bmatrix}, \bar{C}(k) = \begin{bmatrix} C(k) & 0 & 0 \end{bmatrix}, \\
\bar{L}(k) &= L(k)(I - \bar{\Phi}), \quad \bar{\Phi} = \frac{a}{N} I, \\
\bar{\Gamma} &= \mathrm{diag}_{1 \le i \le N}\{\beta_i\}, \quad \tilde{\alpha} = (\theta + \varpi)\alpha^2.
\end{aligned}$$

**Proof.** Define

$$\mathscr{R}(k) = \eta^T(k)R(k)\eta(k), \tag{11}$$

$$J_1(k) = \mathscr{R}(k+1) - \mathscr{R}(k). \tag{12}$$

Similarly to the employment of Lemma 1 in [48], it can be derived from $\mathbb{E}\{\tilde{\Gamma}\} = 0$ and $\mathbb{E}\{\Phi_{\sigma(k)}\} = \bar{\Phi}$. Incorporating the zero term

$$\mathbb{E}\Big\{ \mathcal{J}_1(k) + \alpha^2\|\xi(k)\|^2 + \gamma^2\|v(k)\|^2 - \|\tilde{z}(k)\|^2 - \alpha^2\|\xi(k)\|^2 \Big\}$$

and considering

$$\xi^T(k)\xi(k) \le (\theta\delta(k) + \varpi)y^T(k)y(k), \tag{13}$$

we obtain

$$\begin{aligned}
\mathbb{E}\{J_1(k)\} \le \mathbb{E}\Big\{ & \eta^T(k)\big(\Pi_{1,k+1} + \mathcal{H}^T(k)\mathcal{H}(k) + \tilde{\alpha}\bar{C}^T(k)\bar{C}(k) - R(k)\big)\eta(k) \\
& - \xi^T(k)\Omega_{1,k+1}\xi(k) - v^T(k)\Big( \gamma^2 I - \tilde{\mathcal{B}}^T(k)R(k+1)\tilde{\mathcal{B}}(k) \\
& - \tilde{\alpha}D^T(k)D(k) \Big) v(k) + 2\eta^T(k)\Big( \tilde{\mathcal{A}}^T(k)R(k+1)\tilde{\mathcal{B}}(k) \\
& + \Pi_{2,k+1} + \tilde{\alpha}\bar{C}(k)D(k) \Big) v(k) - \mathcal{J}_1(k) \Big\}
\end{aligned} \tag{14}$$

where

$$\begin{aligned}
\Pi_{1,k+1} &= \tilde{\mathcal{A}}^T(k)R(k+1)\tilde{\mathcal{A}}(k) + \tilde{\mathcal{W}}^T(k)R(k+1)\tilde{\mathcal{W}}(k), \\
\Pi_{2,k+1} &= 2\eta^T(k)\tilde{\mathcal{A}}^T(k)R(k+1)\tilde{C}(k)\xi(k) + 2\xi^T(k)\tilde{C}^T(k)R(k+1)\tilde{\mathcal{B}}(k)v(k).
\end{aligned}$$

Utilizing the technique of completing the square, we obtain

$$-\xi^T(k)\Omega_{1,k+1}\xi(k)+\Pi_{2,k+1}=\bar{\xi}^T(k)\Omega_{1,k+1}\bar{\xi}(k)-\tilde{\xi}^T(k)\Omega_{1,k+1}\tilde{\xi}(k) \tag{15}$$

where

$$\bar{\xi}(k)=\xi(k)-\tilde{\xi}(k),$$
$$\tilde{\xi}(k)=\Omega_{1,k+1}^{-1}\tilde{C}^T(k)R(k+1)\big(\tilde{\mathcal{A}}(k)\eta(k)+\tilde{\mathcal{B}}(k)v(k)\big).$$

Substituting (15) into (14) yields

$$\begin{aligned}\mathbb{E}\{J_1(k)\}\le\mathbb{E}\Big\{&\eta^T(k)\big(\Pi_{3,k+1}-R(k)\big)\eta(k)-v^T(k)\Omega_{2,k+1}v(k)+\Pi_{4,k+1}\\&-\bar{\xi}^T(k)\Omega_{1,k+1}\bar{\xi}(k)-\mathcal{J}_1(k)\Big\}\end{aligned} \tag{16}$$

where

$$\Pi_{4,k+1}=2\eta^T(k)\big(\tilde{\mathcal{A}}^T(k)\Xi_{k+1}\tilde{\mathcal{B}}(k)+\tilde{\alpha}\tilde{C}^T(k)D(k)\big)v(k).$$

Similar to (15), we have

$$-v^T(k)\Omega_{2,k+1}v(k)+\Pi_{4,k+1}=\tilde{v}^T(k)\Omega_{2,k+1}\tilde{v}(k)-\bar{v}^T(k)\Omega_{2,k+1}\bar{v}(k) \tag{17}$$

where

$$\bar{v}(k)=v(k)-\tilde{v}(k),\quad \tilde{v}(k)=\Omega_{2,k+1}^{-1}\Theta_{1,k+1}\eta(k).$$

Substituting (17) into (16) yields

$$\begin{aligned}\mathbb{E}\{J_1(k)\}\le\mathbb{E}\Big\{&\eta^T(k)\big(\Pi_{3,k+1}+\Theta_{1,k+1}^T\Omega_{2,k+1}^{-1}\Theta_{1,k+1}-R(k)\big)\eta(k)\\&-\bar{\xi}^T(k)\Omega_{1,k+1}\bar{\xi}(k)-\tilde{v}^T(k)\Omega_{2,k+1}\tilde{v}(k)-\mathcal{J}_1(k)\Big\}.\end{aligned} \tag{18}$$

Accumulating the sum from 0 to $T$ on both sides of (18) with (12), one obtains

$$\begin{aligned}&\mathbb{E}\big\{\mathscr{R}(k+1)-\mathscr{R}(0)\big\}\\&\le\mathbb{E}\Big\{-\sum_{k=0}^{T}\Big(\mathcal{J}_1(k)+\bar{\xi}^T(k)\Omega_{1,k+1}\bar{\xi}(k)+\tilde{v}^T(k)\Omega_{2,k+1}\tilde{v}(k)\Big)\Big\}.\end{aligned} \tag{19}$$

Considering the condition (10) and $R(T+1)=0$, we can obtain

$$\mathbb{E}\Big\{\sum_{k=0}^{T}\mathcal{J}_1(k)\Big\}<\eta^T(0)S\eta(0). \tag{20}$$

Based on the definition of $H_\infty$ performance in (8), it follows from (20) that (6) satisfies the $H_\infty$ estimation performance. Afterwards, we will obtain the gain $L(k)$ under the most unfavorable circumstances. Suppose that

$$\xi(k)=\tilde{\xi}(k)=\Omega_{1,k+1}^{-1}\Theta_{2,k+1}\eta(k), \tag{21}$$

$$v(k)=\tilde{v}(k)=\Omega_{2,k+1}^{-1}\Theta_{1,k+1}\eta(k) \tag{22}$$

where

$$\Theta_{2,k+1}=\tilde{C}^T(k)R(k+1)\big(\tilde{\mathcal{A}}(k)+\tilde{\mathcal{B}}(k)\Omega_{2,k+1}^{-1}\Theta_{1,k+1}\big).$$

Substituting (21) and (22) into (7) yields

$$\begin{cases}\eta(k+1)=\big(\hat{\mathcal{A}}(k)+\mathcal{W}(k)+\mathcal{C}(k)\Omega_{1,k+1}^{-1}\Theta_{2,k+1}\\\qquad\qquad+\mathcal{B}(k)\Omega_{2,k+1}^{-1}\Theta_{1,k+1}\big)\eta(k)+\mathcal{I}\psi(k)\\\tilde{z}(k)=\mathcal{H}(k)\eta(k)\end{cases} \tag{23}$$

where

$$\hat{\mathcal{A}}(k)=\begin{bmatrix}\tilde{A}(k)&0&0\\\Phi_{\sigma(k)}C(k)&I-\Phi_{\sigma(k)}&0\\\tilde{L}(k)C(k)&-\tilde{L}(k)&\tilde{A}(k)\end{bmatrix},$$
$$\mathcal{I}=\begin{bmatrix}0&0&I\end{bmatrix}^T,\quad \hat{C}(k)=\begin{bmatrix}0&0&C(k)\end{bmatrix},\quad \psi(k)=L(k)\hat{C}(k)\eta(k).$$

In view of (21) and (22) under the most unfavorable scenarios, we define the performance index for the system (23) as follows:

$$\mathcal{G}(L(k))=\sum_{k=0}^{T}\mathbb{E}\big\{\mathcal{J}_2(k)\big\} \tag{24}$$

where

$$\mathcal{J}_2(k) = \|\tilde{z}(k)\|^2 + \|\psi(k)\|^2.$$

**Theorem 2.** *Consider the CNs (1) and the estimation error system (7). Assume that there are matrices $R(k) > 0$ and $Q(k) > 0$ such that for given scalars $\gamma > 0$, $\alpha > 0$, matrix $S^T = S > 0$, and the estimator gain $L(k)$, the BDEs hold for $k \in [0, T]$:*

$$Q(k) = \Lambda_{2,k+1} - \Lambda_{3,k+1}\Omega_{3,k+1}^{-1}\Lambda_{3,k+1}^T \tag{25}$$

*with*

$$R(T+1) = 0, \quad Q(T+1) = 0, \tag{26}$$

*the conditions (10) and*

$$\Omega_{3,k+1} > 0 \tag{27}$$

*where*

$$\begin{aligned}
&\Lambda_{1,k+1} = \tilde{\Psi}_{k+1}^T Q(k+1)\tilde{\Psi}_{k+1} + \tilde{\mathcal{W}}^T(k)Q(k+1)\tilde{\mathcal{W}}(k),\\
&\Lambda_{2,k+1} = \Lambda_{1,k+1} + \mathcal{H}^T(k)\mathcal{H}(k) + 2\Psi_{k+1}^T Q(k+1)\mathcal{I}L(k)\hat{C}(k),\\
&\Lambda_{3,k+1} = \bar{\mathcal{A}}^T(k)Q(k+1)\mathcal{I},\\
&\Psi_{k+1} = \tilde{C}(k)\Omega_{1,k+1}^{-1}\Theta_{2,k+1} + \tilde{B}(k)\Omega_{2,k+1}^{-1}\Theta_{1,k+1},\\
&\Omega_{3,k+1} = \mathcal{I}^T Q(k+1)\mathcal{I} + I, \quad \tilde{\Psi}_{k+1} = \bar{\mathcal{A}}(k) + \Psi_{k+1},\\
&\bar{\mathcal{A}}(k) = \begin{bmatrix} \tilde{A}(k) & 0 & 0\\ \bar{\Phi}C(k) & I - \bar{\Phi} & 0\\ \bar{L}C(k) & -\bar{L}(k) & \tilde{A}(k) \end{bmatrix}.
\end{aligned}$$

**Proof.** Define

$$\mathcal{Q}(k) = \eta^T(k)Q(k)\eta(k), \tag{28}$$

$$J_2(k) = \mathcal{Q}(k+1) - \mathcal{Q}(k). \tag{29}$$

Similar to Theorem 1, one has

$$\begin{aligned}
\mathbb{E}\{J_2(k)\} = \mathbb{E}\Big\{ &\eta^T(k)\big(\Lambda_{1,k+1} - Q(k)\big)\eta(k) + 2\eta^T(k)\tilde{\Psi}_{k+1}^T Q(k+1)\mathcal{I}\psi(k)\\
&+ \psi^T(k)\mathcal{I}^T Q(k+1)\mathcal{I}\psi(k)\Big\}.
\end{aligned} \tag{30}$$

Incorporating the zero term

$$\mathbb{E}\Big\{\|\tilde{z}(k)\|^2 + \|\psi(k)\|^2 - \mathcal{J}_2(k)\Big\}$$

into (30), we get

$$\begin{aligned}
\mathbb{E}\{J_2(k)\} = \mathbb{E}\Big\{ &\eta^T(k)\big(\Lambda_{2,k+1} - Q(k)\big)\eta(k) + 2\eta^T(k)\\
&\times \Lambda_{3,k+1} + \psi^T(k)\Omega_{3,k+1}\psi(k) - \mathcal{J}_2(k)\Big\}.
\end{aligned} \tag{31}$$

Implementing the method of square completion, it follows that

$$2\eta^T(k)\Lambda_{3,k+1} + \psi^T(k)\Omega_{3,k+1}\psi(k) = -\tilde{\psi}^T(k)\Omega_{3,k+1}\tilde{\psi}(k) + \bar{\psi}^T(k)\Omega_{3,k+1}\bar{\psi}(k) \tag{32}$$

where

$$\bar{\psi}(k) = \psi(k) + \tilde{\psi}(k), \quad \tilde{\psi}(k) = \Omega_{3,k+1}^{-1}\Lambda_{3,k+1}^T\eta(k).$$

Based on (32), one has

$$\begin{aligned}
\mathbb{E}\{J_2(k)\} = \mathbb{E}\Big\{ &\eta^T(k)\big(\Lambda_{2,k+1} - \Lambda_{3,k+1}\Omega_{3,k+1}^{-1}\Lambda_{3,k+1}^T\\
&- Q(k)\big)\eta(k) + \bar{\psi}^T(k)\Omega_{3,k+1}\bar{\psi}(k) - \mathcal{J}_2(k)\Big\}.
\end{aligned}$$

Similar to (19), we have

$$\begin{aligned}
\mathcal{G}(L(k)) - \mathcal{Q}(0) &= \mathbb{E}\Big\{\sum_{k=0}^{T}\bar{\psi}^T(k)\Omega_{3,k+1}\bar{\psi}(k)\Big\}\\
&\le \mathbb{E}\Big\{\sum_{k=0}^{T}\|\eta(k)\|^2\|\mathcal{L}(k)\|_F^2\|\Omega_{3,k+1}\|_F^2\Big\}
\end{aligned} \tag{33}$$

where

$$\mathcal{L}(k) = L(k)\hat{C}(k) + P(k), \quad P(k) = \Omega_{3,k+1}^{-1} A_{3,k+1}^{T}.$$

It can be inferred from (33) that the performance index $\mathcal{G}(L(k))$ can be minimized by adjusting gain matrix $L(k)$.

**Theorem 3.** *Consider the CNs (1) and the estimation error system (7). Given $\gamma > 0$, $\alpha > 0$, and matrix $S^T = S > 0$, if there exist matrices $R(k) > 0$ and $Q(k) > 0$ such that the BDEs (9) and (25) hold with (26), (10), and (27), the gain of (6) is determined by*

$$L(k) = -\tilde{P}(k)C^{+}(k) \tag{34}$$

*where $\tilde{P}(k)$ represents the third block element of $P(k)$ and $C^{+}(k)$ denotes the Moore–Penrose pseudoinverse of $C(k)$.*

**Proof.** From (33), we can deduce that minimizing the performance metric $\mathcal{G}(L(k))$ can be transformed into minimizing $\|\mathcal{L}(k)\|_F^2$. Further derivation leads us to obtain

$$L(k)C(k) = -\tilde{P}(k). \tag{35}$$

Furthermore, we get (34).

**Remark 5.** Through the analysis of Theorems 1 and 2, adequate conditions guaranteeing the estimator $H_\infty$ performance are obtained for CNs under the influence of ICD, AFETM, and MRAP. Based on this, Theorem 3 provides specific methods for calculating the estimator gain during the process of solving the BDEs. This calculation process incorporates all the key information necessary to guarantee the estimator $H_\infty$ performance, including the system parameter, statistical characteristics of ICD, relevant parameters of AFETM, scheduling matrix of MRAP, and $H_\infty$ performance indicators.

## 4. Numerical example

This section demonstrates the effectiveness of the devised estimator by one numerical instance.

Consider the CNs (1) consisting of five nodes, its parameters are specified as follows:

$$A_1(k) = \begin{bmatrix} 0.41 + 0.82\sin(k) & 0.21 \\ -0.60 & 0.81 - 0.65\cos(k) \end{bmatrix},$$

$$A_2(k) = \begin{bmatrix} 0.75 + 0.29\sin(k) & 0.26 \\ -0.65 & 0.78 + 0.64\cos(k) \end{bmatrix},$$

$$A_l(k) = \begin{bmatrix} 0.65 + 0.26\cos(k) & -0.46 \\ 0.25 & 0.77 + 0.62\sin(k) \end{bmatrix},$$

$$B_1(k) = \begin{bmatrix} 0.06 + 0.1\cos(k) \\ 0.18 \end{bmatrix}, B_2(k) = \begin{bmatrix} 0.13 + 0.2\sin(k) \\ 0.21 \end{bmatrix},$$

$$B_l(k) = \begin{bmatrix} 0.12 \\ 0.21 + 0.2\sin(k) \end{bmatrix},$$

$$C_1(k) = \begin{bmatrix} 0.32 & 0.62 + 0.4\cos(0.3k) \end{bmatrix},$$

$$C_2(k) = \begin{bmatrix} 0.32 & 0.39 + 0.3\cos(0.5k) \end{bmatrix},$$

$$C_l(k) = \begin{bmatrix} 0.25 & 0.48 + 0.1\cos(0.2k) \end{bmatrix},$$

$$H_1(k) = \begin{bmatrix} 0.12\sin(k) & 0.10\sin(k) \end{bmatrix},$$

$$H_2(k) = \begin{bmatrix} 0.21\cos(k) & 0.11\cos(k) \end{bmatrix},$$

$$H_l(k) = \begin{bmatrix} 0.20\sin(k) & 0.12\cos(k) \end{bmatrix}, \quad l = 3, 4, 5.$$

$$W = \begin{bmatrix} -0.35 & 0.08 & 0.09 & 0.08 & 0.10 \\ 0.08 & -0.40 & 0.11 & 0.09 & 0.12 \\ 0.09 & 0.11 & -0.33 & 0.07 & 0.06 \\ 0.08 & 0.09 & 0.07 & -0.32 & 0.08 \\ 0.10 & 0.12 & 0.06 & 0.08 & -0.36 \end{bmatrix},$$

$\Gamma = \mathrm{diag}\{0.2, 0.3\}$, and the variance of ICD is $\bar{\Gamma} = \mathrm{diag}\{0.04, 0.05\}$.

The parameters related to AFETM are $\theta = 0.12$, $\varpi = 0.20$, $r = 2$, $p = 5$, and the initial threshold $\delta(0) = 0.5$. In each scheduling of MRAP, the number of randomly selected nodes for transmission is $a = 2$. The scalars $\gamma = 1.20$, $\alpha = 0.40$, and $S = 3I$. The external disturbances are $\upsilon_i(k) = 0.05\cos(0.87k), (i = 1, 2, \ldots, 5)$.

The initial states are set as $x_1(0) = \begin{bmatrix} 0.22 & 0.23 \end{bmatrix}^{\mathrm{T}}$, $x_2(0) = \begin{bmatrix} 0.22 & 0.13 \end{bmatrix}^{\mathrm{T}}$, $x_3(0) = \begin{bmatrix} 0.21 & 0.12 \end{bmatrix}^{\mathrm{T}}$, $x_4(0) = \begin{bmatrix} 0.13 & 0.23 \end{bmatrix}^{\mathrm{T}}$, $x_5(0) = \begin{bmatrix} 0.27 & 0.26 \end{bmatrix}^{\mathrm{T}}$.

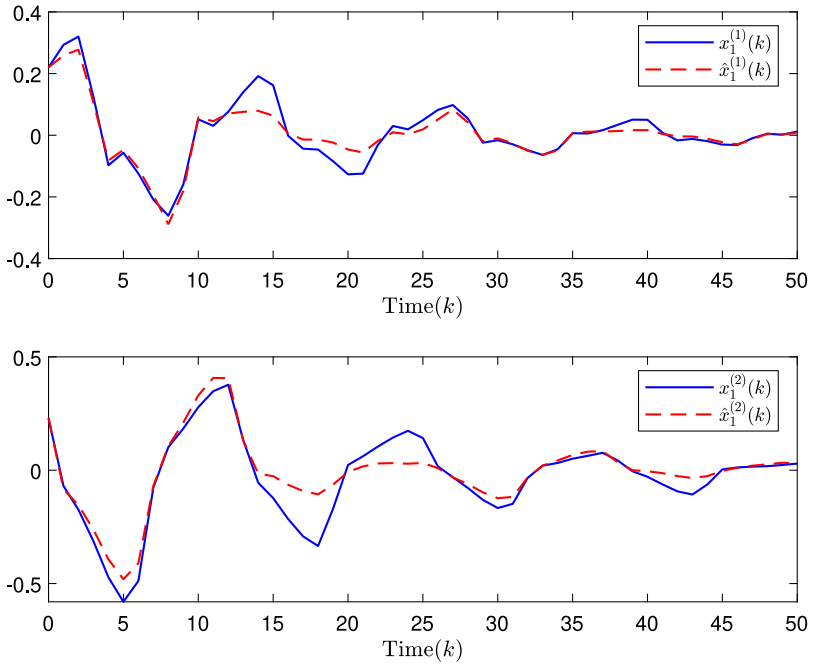


**Fig. 1.** Trajectories of $x_1(k)$ and $\hat{x}_1(k)$.

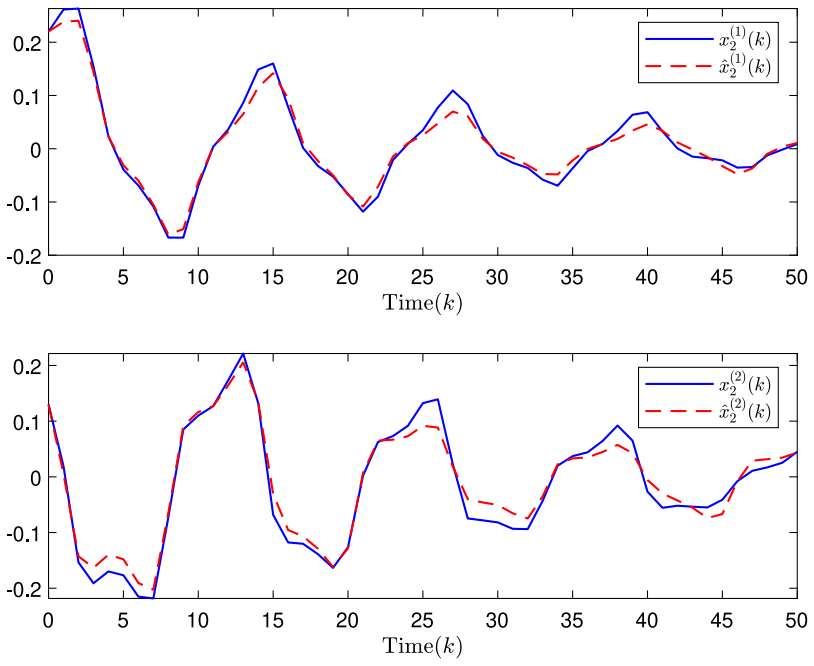


**Fig. 2.** Trajectories of $x_2(k)$ and $\hat{x}_2(k)$.

The system state $x(k)$ and the estimation $\hat{x}(k)$ are displayed in Figs. 1–3. Fig. 4 plots the output estimation error $\tilde{z}(k)$. In Fig. 5, the selected nodes under MRAP can be observed. There are a total of five sensor nodes that need to transmit measurement data. At each sampling instant, the MRAP randomly selects the measurement outputs of two of these sensor nodes for transmission.

The triggering instants of AFETM are presented in Fig. 6. The estimation errors $e_1(k)$ and $e_2(k)$ are shown in Figs. 7–8, which indicates that in the majority of moments, AFETM can achieve smaller estimation errors compared to the existing ETM

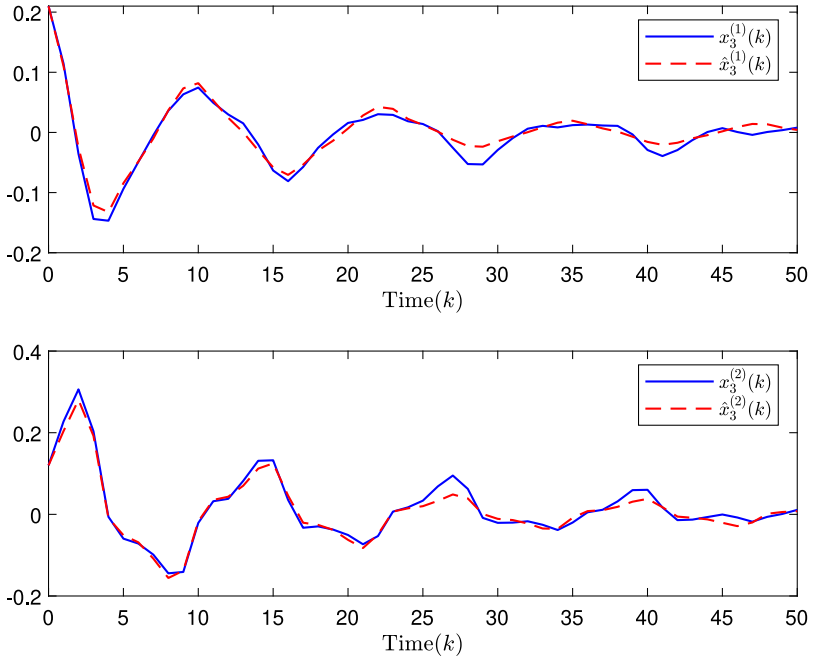


**Fig. 3.** Trajectories of $x_3(k)$ and $\hat{x}_3(k)$.

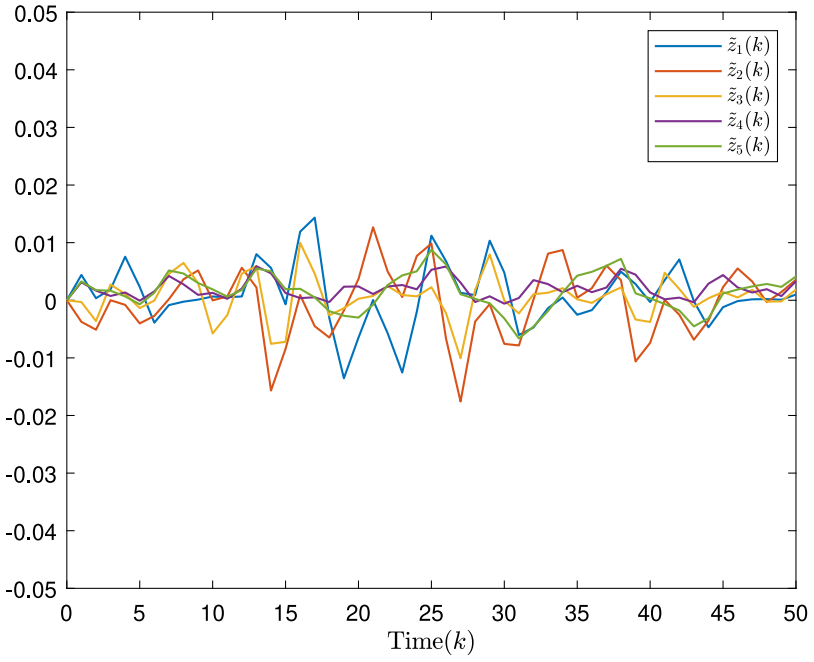


**Fig. 4.** Output estimation error $\tilde{z}(k)$.

in [32,33]. The enhanced AFETM demonstrates better overall estimation performance when compared to the conventional ETM. The aforementioned results provide affirmation that the proposed AFETM is indeed efficacious.

## 5. Conclusion

This paper investigates the state estimation of CNs subject to ICD under AFETM and MRAP. An AFETM that can adaptively adjust the threshold to maintain a stable transmission rate is proposed. In order to avoid network conflicts and blockages, MRAP that

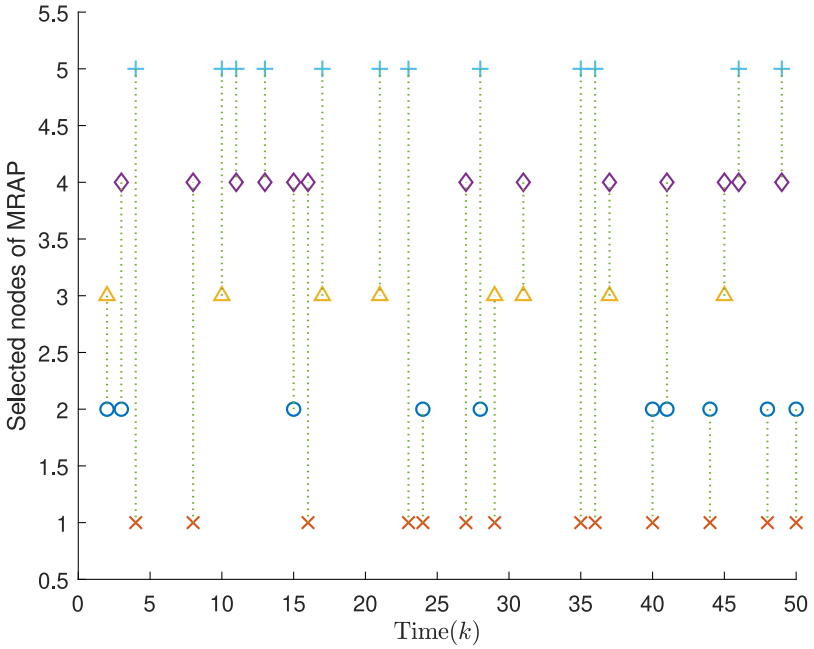


**Fig. 5.** Selected nodes under MRAP.

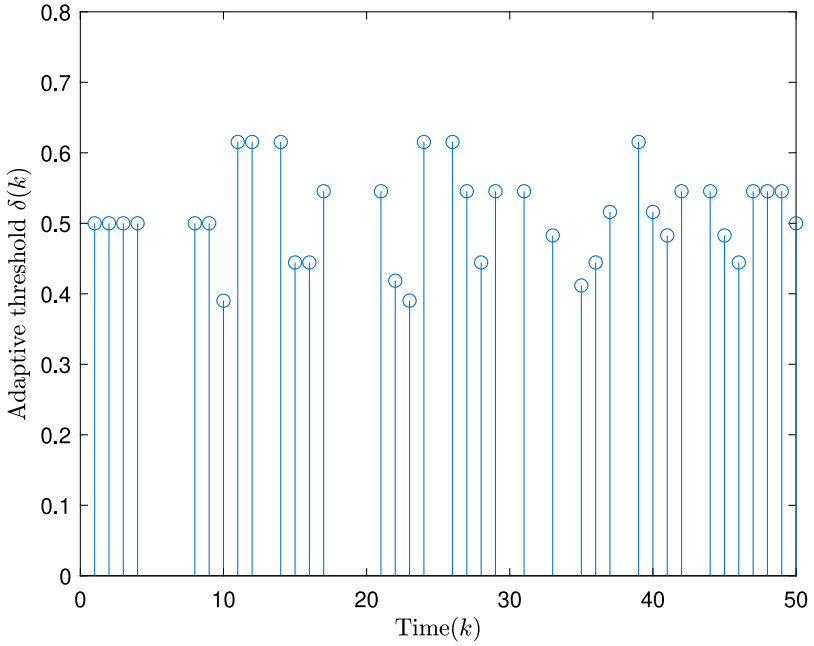


**Fig. 6.** Triggering instants of AFETM.

can randomly select and send multiple measuring signals is used to schedule signal transmission in the communication network. Sufficient conditions for guaranteeing that the dynamic estimation errors satisfy the $H_\infty$ performance are obtained through the utilization of random analysis techniques. The estimator gain that can make the CNs achieve the expected system performance have been derived by solving the BDEs. Ultimately, the feasibility of the devised estimator is verified through simulation results. Our future work would include the privacy-preserving state estimation of resource-constrained CNs subject to eavesdropping attacks.

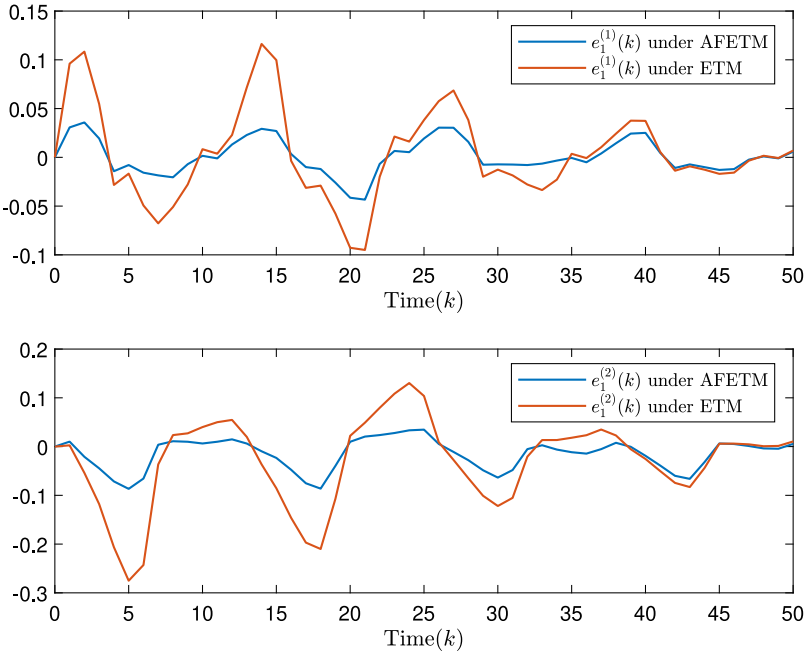


**Fig. 7.** Estimation error $e_1(k)$ under AFETM and ETM.

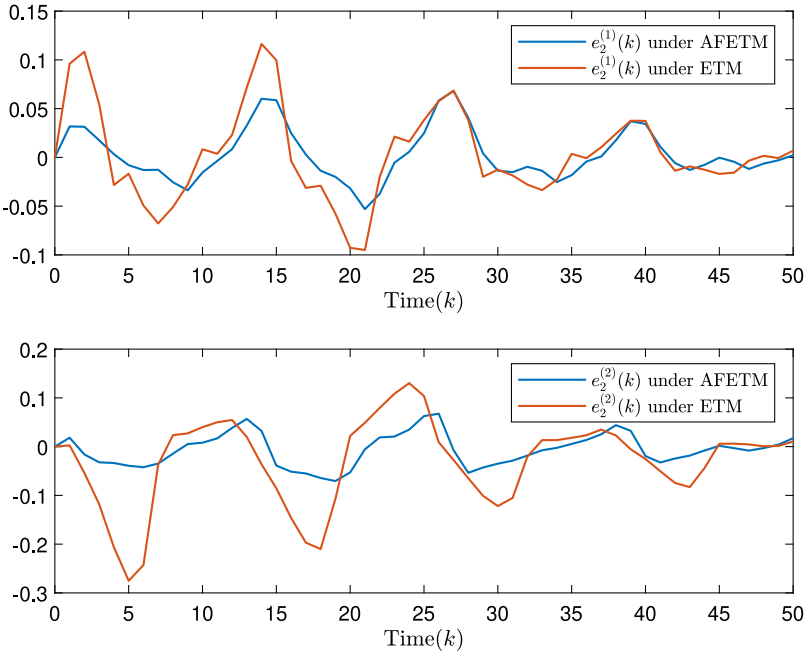


**Fig. 8.** Estimation error $e_2(k)$ under AFETM and ETM.

## Declaration of competing interest

The authors declare that they have no known competing financial interests or personal relationships that could have appeared to influence the work reported in this paper.

## Acknowledgments

This work was supported in part by the National Natural Science Foundation of China under Grant 62273174 and Grant 61903182, in part by the Natural Science Foundation of Jiangsu Province of China under Grant BK20230063 and in part by the Qing Lan Project, China.

## References

[1] Y. Wu, X. Wang, G.-P. Jiang, M. Gu, Target layer state estimation in multilayer complex dynamical networks using functional observability, J. Franklin Inst. 360 (12) (2023) 8178–8199, http://dx.doi.org/10.1016/j.jfranklin.2023.06.033.
[2] Y. Cui, L. Yu, Y. Liu, W. Zhang, F.E. Alsaadi, Dynamic event-based non-fragile state estimation for complex networks via partial nodes information, J. Franklin Inst. 358 (18) (2021) 10193–10212, http://dx.doi.org/10.1016/j.jfranklin.2021.10.038.
[3] X. Guo, J. Xia, H. Shen, C. Yan, X. Wang, T. Liu, Synchronization of time-delayed complex networks with delay-partitioning: A Chua's circuit networks application, J. Franklin Inst. 360 (18) (2023) 14208–14221, http://dx.doi.org/10.1016/j.jfranklin.2023.10.027.
[4] W. Song, Z. Wang, Z. Li, H. Dong, Q.-L. Han, Protocol-based particle filtering for nonlinear complex networks: Handling non-Gaussian noises and measurement censoring, IEEE Trans. Netw. Sci. Eng. 10 (1) (2023) 128–139, http://dx.doi.org/10.1109/TNSE.2022.3205553.
[5] Z.-H. Pang, C.-G. Xia, J. Zhang, Q.-L. Han, G.-P. Liu, A prediction-based approach realizing finite-time convergence of networked control systems, IEEE Trans. Circuits Syst. II 70 (7) (2023) 2445–2449, http://dx.doi.org/10.1109/TCSII.2023.3235462.
[6] W. Chen, Z. Wang, D. Ding, X. Yi, Q.-L. Han, Distributed state estimation over wireless sensor networks with energy harvesting sensors, IEEE Trans. Cybern. 53 (5) (2023) 3311–3324, http://dx.doi.org/10.1109/TCYB.2022.3179280.
[7] X.-M. Zhang, Q.-L. Han, X. Ge, B.-L. Zhang, Delay-variation-dependent criteria on extended dissipativity for discrete-time neural networks with time-varying delay, IEEE Trans. Neural Netw. Learn. Syst. 34 (3) (2023) 1578–1587, http://dx.doi.org/10.1109/TNNLS.2021.3105591.
[8] Y. Wu, H. Guo, L. Xue, N. Gunasekaran, J. Liu, Prescribed-time synchronization of stochastic complex networks with high-gain coupling, IEEE Trans. Circuits Syst. II 70 (11) (2023) 4133–4137, http://dx.doi.org/10.1109/TCSII.2023.3271150.
[9] L. Sheng, S. Liu, M. Gao, W. Huai, D. Zhou, Moving horizon fault estimation for nonlinear stochastic systems with unknown noise covariance matrices, IEEE Trans. Instrum. Meas. 73 (3502913) (2024) http://dx.doi.org/10.1109/TIM.2023.3331435.
[10] L. Sheng, Y. Niu, W. Wang, M. Gao, Y. Geng, D. Zhou, Estimation of toolface for dynamic point-the-bit rotary steerable systems via nonlinear polynomial filtering, IEEE Trans. Ind. Electron. 69 (7) (2022) 7192–7201, http://dx.doi.org/10.1109/TIE.2021.3097601.
[11] Z.-G. Wu, Z. Xu, P. Shi, M.Z.Q. Chen, H. Su, Nonfragile state estimation of quantized complex networks with switching topologies, IEEE Trans. Neural Netw. Learn. Syst. 29 (10) (2018) 5111–5121, http://dx.doi.org/10.1109/TNNLS.2018.2790982.
[12] H. Dong, N. Hou, Z. Wang, W. Ren, Variance-constrained state estimation for complex networks with randomly varying topologies, IEEE Trans. Neural Netw. Learn. Syst. 29 (7) (2018) 2757–2768, http://dx.doi.org/10.1109/TNNLS.2017.2700331.
[13] L. Liang, J. Cheng, J. Cao, Z.-G. Wu, W.-H. Chen, Proportional–Integral observer-based state estimation for singularly perturbed complex networks with cyberattacks, IEEE Trans. Neural Netw. Learn. Syst. 34 (12) (2023) 9795–9805, http://dx.doi.org/10.1109/TNNLS.2022.3160627.
[14] L. Sheng, Y. Niu, L. Zou, Y. Liu, F.E. Alsaadi, Finite-horizon state estimation for time-varying complex networks with random coupling strengths under Round–Robin protocol, J. Franklin Inst. 355 (15) (2018) 7417–7442, http://dx.doi.org/10.1016/j.jfranklin.2018.07.026.
[15] S. Zhai, X.-S. Yang, Contraction analysis of synchronization of complex switched networks with different inner coupling matrices, J. Franklin Inst. 350 (10) (2013) 3116–3127, http://dx.doi.org/10.1016/j.jfranklin.2013.06.016.
[16] Q. Dong, P. Yu, Y. Ma, Event-triggered synchronization control of complex networks with adaptive coupling strength, J. Franklin Inst. 359 (2) (2022) 1215–1234, http://dx.doi.org/10.1016/j.jfranklin.2021.11.007.
[17] L. Zhang, H. Zhang, H. Yang, Z. Liu, F. Cheng, An interactive co-evolutionary framework for multi-objective critical node detection on large-scale complex networks, IEEE Trans. Netw. Sci. Eng. 10 (3) (2023) 1722–1735, http://dx.doi.org/10.1109/TNSE.2023.3234152.
[18] S. Zhu, J. Zhou, Q. Zhu, N. Li, J.-A. Lu, Adaptive exponential synchronization of complex networks with nondifferentiable time-varying delay, IEEE Trans. Neural Netw. Learn. Syst. 34 (10) (2023) 8124–8130, http://dx.doi.org/10.1109/TNNLS.2022.3145843.
[19] J. Hu, Z. Wang, G.-P. Liu, H. Zhang, Variance-constrained recursive state estimation for time-varying complex networks with quantized measurements and uncertain inner coupling, IEEE Trans. Neural Netw. Learn. Syst. 31 (6) (2020) 1955–1967, http://dx.doi.org/10.1109/TNNLS.2019.2927554.
[20] H. Gao, H. Dong, Z. Wang, F. Han, An event-triggering approach to recursive filtering for complex networks with state saturations and random coupling strengths, IEEE Trans. Neural Netw. Learn. Syst. 31 (10) (2020) 4279–4289, http://dx.doi.org/10.1109/TNNLS.2019.2953649.
[21] D. Yue, E. Tian, Q.-L. Han, A delay system method for designing event-triggered controllers of networked control systems, IEEE Trans. Automat. Control 58 (2) (2013) 475–481, http://dx.doi.org/10.1109/TAC.2012.2206694.
[22] D. Yue, Q.-L. Han, J. Lam, Network-based robust $H_\infty$ control of systems with uncertainty, Automatica 41 (6) (2005) 999–1007, http://dx.doi.org/10.1016/j.automatica.2004.12.011.
[23] H. Lu, Y. Hu, C. Guo, W. Zhou, Cluster synchronization for a class of complex dynamical network system with randomly occurring coupling delays via an improved event-triggered pinning control approach, J. Franklin Inst. 357 (4) (2020) 2167–2184, http://dx.doi.org/10.1016/j.jfranklin.2019.11.076.
[24] M. Gao, W. Huai, L. Sheng, D. Zhou, Dynamic event-triggered intermittent fault detection for time-varying stochastic systems, IEEE Trans. Ind. Electron. 71 (3) (2024) 3074–3082, http://dx.doi.org/10.1109/TIE.2023.3270510.
[25] J. Liu, N. Zhang, Y. Li, X. Xie, E. Tian, J. Cao, Learning-based event-triggered tracking control for nonlinear networked control systems with unmatched disturbance, IEEE Trans. Syst. Man Cybern. Syst. 53 (5) (2023) 3230–3240, http://dx.doi.org/10.1109/TSMC.2022.3224432.
[26] L. Zha, R. Liao, J. Liu, X. Xie, E. Tian, J. Cao, Outlier-resistant distributed filtering over sensor networks under dynamic event-triggered schemes and DoS attacks, IEEE Trans. Autom. Sci. Eng. (2024) http://dx.doi.org/10.1109/TASE.2024.3360718.
[27] L. Zha, R. Liao, J. Liu, X. Xie, E. Tian, J. Cao, Dynamic event-triggered output feedback control for networked systems subject to multiple cyber attacks, IEEE Trans. Cybern. 52 (12) (2022) 13800–13808, http://dx.doi.org/10.1109/TCYB.2021.3125851.
[28] Y. Liu, Z. Wang, L. Zou, J. Hu, H. Dong, Distributed filtering for complex networks under multiple event-triggered transmissions within node-wise communications, IEEE Trans. Netw. Sci. Eng. 9 (4) (2022) 2521–2534, http://dx.doi.org/10.1109/TNSE.2022.3164833.
[29] Y. Ju, D. Ding, X. He, Q.-L. Han, G. Wei, Consensus control of multi-agent systems using fault-estimation-in-the-loop: Dynamic event-triggered case, IEEE/CAA J. Autom. Sin. 9 (8) (2022) 1440–1451, http://dx.doi.org/10.1109/JAS.2021.1004386.
[30] S. Xiao, X. Ge, Q.-L. Han, Y. Zhang, Dynamic event-triggered platooning control of automated vehicles under random communication topologies and various spacing policies, IEEE Trans. Cybern. 52 (11) (2022) 11477–11490, http://dx.doi.org/10.1109/TCYB.2021.3103328.
[31] X. Ge, S. Xiao, Q.-L. Han, X.-M. Zhang, D. Ding, Dynamic event-triggered scheduling and platooning control co-design for automated vehicles over vehicular ad-hoc networks, IEEE/CAA J. Autom. Sin. 9 (1) (2022) 31–46, http://dx.doi.org/10.1109/JAS.2021.1004060.
[32] X. Ruan, J. Feng, C. Xu, J. Wang, Y. Zhao, Dynamic event-triggered pinning synchronization for switched impulsive complex networks with asynchronous switching, IEEE Trans. Circuits Syst. II 69 (4) (2022) 2211–2215, http://dx.doi.org/10.1109/TCSII.2021.3123285.

[33] Q. Li, Z. Wang, N. Li, W. Sheng, A dynamic event-triggered approach to recursive filtering for complex networks with switching topologies subject to random sensor failures, IEEE Trans. Neural Netw. Learn. Syst. 31 (10) (2020) 4381–4388, http://dx.doi.org/10.1109/TNNLS.2019.2951948.
[34] D. Yue, Q.-L. Han, C. Peng, State feedback controller design of networked control systems, IEEE Trans. Circuits Syst. II 51 (11) (2004) 640–644, http://dx.doi.org/10.1109/TCSII.2004.836043.
[35] Y. Luo, Z. Wang, Y. Chen, X. Yi, $H_\infty$ State estimation for coupled stochastic complex networks with periodical communication protocol and intermittent nonlinearity switching, IEEE Trans. Netw. Sci. Eng. 8 (2) (2021) 1414–1425, http://dx.doi.org/10.1109/TNSE.2021.3058220.
[36] L. Zha, Y. Guo, J. Liu, X. Xie, E. Tian, Protocol-based distributed security fusion estimation for time-varying uncertain systems over sensor networks: Tackling DoS attacks, IEEE Trans. Signal Inf. Process. Over Netw. 10 (2024) 119–130, http://dx.doi.org/10.1109/TSIPN.2024.3356789.
[37] H. Shen, S. Huo, J. Cao, T. Huang, Generalized state estimation for Markovian coupled networks under Round–Robin protocol and redundant channels, IEEE Trans. Cybern. 49 (4) (2019) 1292–1301, http://dx.doi.org/10.1109/TCYB.2018.2799929.
[38] L. Zou, Z. Wang, Q.-L. Han, D. Zhou, Moving horizon estimation of networked nonlinear systems with random access protocol, IEEE Trans. Syst. Man Cybern. Syst. 51 (5) (2021) 2937–2948, http://dx.doi.org/10.1109/TSMC.2019.2918002.
[39] L. Zou, Z. Wang, Q.-L. Han, D. Zhou, Recursive filtering for time-varying systems with random access protocol, IEEE Trans. Automat. Control 64 (2) (2019) 720–727, http://dx.doi.org/10.1109/TAC.2018.2833154.
[40] J. Liu, E. Gong, L. Zha, X. Xie, E. Tian, Outlier-resistant recursive security filtering for multirate networked systems under fading measurements and Round–Robin protocol, IEEE Trans. Control Netw. Syst. 10 (4) (2023) 1962–1974, http://dx.doi.org/10.1109/TCNS.2023.3256299.
[41] J. Song, Z. Wang, Y. Niu, X. Yi, Q.-L. Han, Co-design of dissipative deconvolution filter and Round–Robin protocol for networked 2-D digital systems: Optimization and application, IEEE Trans. Syst. Man Cybern. Syst. 53 (10) (2023) 6316–6328, http://dx.doi.org/10.1109/TSMC.2023.3284223.
[42] H. Geng, Z. Wang, J. Hu, Q.-L. Han, Y. Cheng, Variance-constrained filter design with sensor resolution under Round–Robin communication protocol: An outlier-resistant mechanism, IEEE Trans. Syst. Man Cybern. Syst. 53 (6) (2023) 3762–3773, http://dx.doi.org/10.1109/TSMC.2023.3234461.
[43] X. Li, G. Wei, D. Ding, S. Liu, Recursive filtering for time-varying discrete sequential systems subject to deception attacks: Weighted try-once-discard protocol, IEEE Trans. Syst. Man Cybern. Syst. 52 (6) (2022) 3704–3713, http://dx.doi.org/10.1109/TSMC.2021.3064653.
[44] J. Liu, E. Gong, L. Zha, E. Tian, X. Xie, Interval type-2 fuzzy-model-based filtering for nonlinear systems with event-triggering weighted try-once-discard protocol and cyberattacks, IEEE Trans. Fuzzy Syst. 32 (3) (2024) 721–732, http://dx.doi.org/10.1109/TFUZZ.2023.3305088.
[45] T. Fang, T. Ru, D. Fu, L. Su, J. Wang, Extended dissipative filtering for Markov jump BAM inertial neural networks under weighted try-once-discard protocol, J. Franklin Inst. 358 (7) (2021) 4103–4117, http://dx.doi.org/10.1016/j.jfranklin.2021.03.009.
[46] N. Hou, H. Dong, Z. Wang, H. Liu, A partial-node-based approach to state estimation for complex networks with sensor saturations under random access protocol, IEEE Trans. Neural Netw. Learn. Syst. 32 (11) (2021) 5167–5178, http://dx.doi.org/10.1109/TNNLS.2020.3027252.
[47] X. Wan, Z. Wang, M. Wu, X. Liu, $H_\infty$ State estimation for discrete-time nonlinear singularly perturbed complex networks under the Round–Robin protocol, IEEE Trans. Neural Netw. Learn. Syst. 30 (2) (2019) 415–426, http://dx.doi.org/10.1109/TNNLS.2018.2839020.
[48] Y. Chen, Z. Wang, L. Wang, W. Sheng, Finite-horizon $H_\infty$ state estimation for stochastic coupled networks with random inner couplings using Round–Robin protocol, IEEE Trans. Cybern. 51 (3) (2021) 1204–1215, http://dx.doi.org/10.1109/TCYB.2020.3004288.